

PACS numbers: 61.43.Bn, 62.25.Mn

NUMERICAL INVESTIGATION OF THE BOMBARDMENT OF A GRAPHENE SHEET BY A BEAM OF CARBON ATOMS

O.V. Khomenko, M.V. Prodanov, Yu.V. Scherbak

Sumy State University,
2, Rimsky-Korsakov Str., 40007, Sumy, Ukraine
E-mail: khom@mss.sumdu.edu.ua, prodk@rambler.ru

Classical molecular dynamics simulations of the bombardment of a graphene sheet by a beam of carbon atoms are carried out. Covalent bonds in the irradiated sample are described by the Brenner potential. The approximation of elastic balls interacting with graphene via the Lennard-Jones potential is used for particles in a beam. The influence of the energy and density of irradiating carbon atoms and of the presence of a thermostat on physical processes occurring during the collisions with the sample is investigated. Energy values of the particles in a beam, which are enough for the sample destruction, are defined.

Keywords: GRAPHENE, BOMBARDMENT, FRACTURE, THERMOSTAT, MOLECULAR DYNAMICS.

(Received 8 September 2009, in final form 21 October 2009)

1. INTRODUCTION

Recent discovery of graphene was and still is of a great interest, which is mainly focused on the peculiar electronic properties of this material, where charge carriers bear a resemblance to the massless relativistic particles [1-4]. However, the structure of graphene, which is a single layer of carbon atoms densely packed into the hexagonal crystal lattice, has not been completely understood yet. On the one hand, graphene is found to be a strictly two-dimensional material, exhibiting such a high quality of crystal structure that electrons can travel submicron distances without scattering at the room temperature. On the other hand, it was shown theoretically that perfect two-dimensional crystals cannot exist in the free state, and this has been confirmed experimentally for a long time [5-7].

Experiments with the scanning transmission electron microscope (STEM) reveal the existence of isolated point defects in graphene, in particular, the vacancies [8]. Their presence is connected with the crystal structure damage due to irradiation or ion bombardment and because of the interaction with the STEM electron beam as well. Thorough understanding of formation conditions of the graphene defect structure has a big importance for construction of electronic devices on its basis because the crystal lattice quality essentially influences on the electronic properties of this material.

Study of the defect formation in graphene and its damage under different-particle bombardment can be the first step to understanding the process of graphite destruction by the plasma flow, which is of interest during the nuclear fusion investigation [9, 10]. In experimental facilities and thermonuclear reactors the destruction of graphite divertor occurs under plasma flow action. Within the framework of this task a number of computer experiments using classical molecular dynamics (MD) was carried out.

Processes of the graphene sheet bombardment by single atoms of hydrogen isotopes [9] and the graphite sample irradiation by these particles [10] have been studied. In the models the new version of the Brenner potential was used and the microcanonical statistical ensemble was considered. The main result of the cited publications consists in determination of particle energies and masses, at which the particle reflection, absorption or penetration into graphene sheet and the graphite sample destruction occur. But we should note, that the deficiencies of numerical experiments in [9, 10] are the following. First, only the short-range Brenner potential was used for the interactions between irradiating particles and carbon atoms. Second, the single atoms, but not a particle beam, were employed for irradiation that is hardly probable in the experiments. In addition, limitation of the models appears in the absence of energy emission from the system, which always takes place in practice.

The necessity of studying more realistic models, where the disadvantages indicated above are removed, is evident and that is the reason for computer experiments described in the present work. The MD simulations, in which the interaction of a graphene sheet with a flow of carbon atoms is considered, are carried out. Investigation of the influence of energy and particle density in a beam, and of graphene cooling as well on the physical processes during irradiation of the sample is the main aim of the paper. Detailed description of the simulation conditions is given in the next section.

2. THE MODEL

A graphene sheet consists of 24×24 honeycombs translated periodically along the x - and y -axes (Fig. 1). Periodical boundary conditions are applied to the sample in the xy -plane. Carbon layer contains 3456 atoms and its sizes along the x - and y -axes are 10,082 nm and 8,731 nm, respectively.

A beam of carbon atoms is modeled by a set of elastic balls, which form the truncated pyramidal structure and at the start time are placed in the corners of a cubic lattice located over the center of symmetry of the sample. To study the influence of the density of irradiating particles on a system behavior we used the following three values of the cubic lattice constant: $a = 0,3165$ nm, $0,2374$ nm, and $0,1582$ nm. A beam consists of five layers of square section lying in the xy -plane. There are 169 atoms in the lower layer (the nearest to the irradiated sample), and each overlying layer is one line of particles more along the x - and y -axes, thus there are 1135 atoms in a beam, and the total number of particles involved in the simulation is 4591.

The form of the interaction potential between particles [12-15] plays a key role for realistic simulation by the MD method. In the present work the covalent bonds in a graphene sheet are described by the potential developed by Brenner for simulation of hydrocarbons. It is of the form of a sum over all the bonds [16-18]:

$$V_b = \sum_i \sum_{j>i} [V_R(r_{ij}) - \bar{B}_{ij} V_A(r_{ij})]. \quad (1)$$

Functions $V_R(r_{ij})$ and $V_A(r_{ij})$ are the pairwise additive interactions, which represent all interatomic repulsions (between ion cores, etc.) and attractions between valence electrons, respectively; r_{ij} is the distance between pairs of the nearest neighbor atoms i and j ; \bar{B}_{ij} is the term of the bond order

representing the bond type between the i -th and the j -th atoms and containing the many-particle effects, which are necessary for the correct description of bonding in hydrocarbonates.

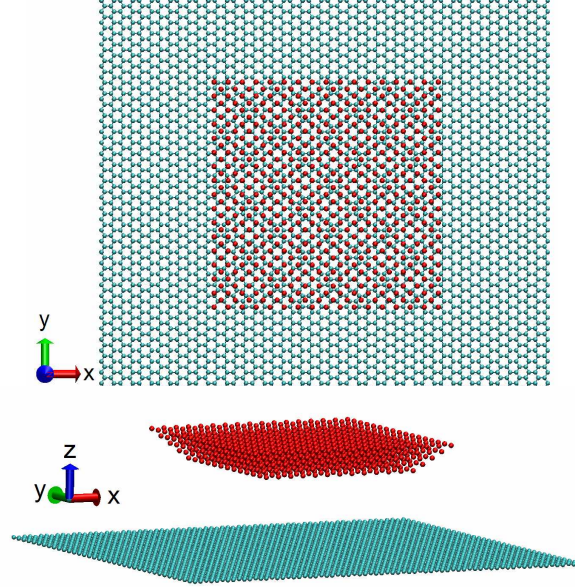


Fig. 1 – Initial system configurations for $a = 0,3165$ nm. Cyanic and red small balls represent the carbon atoms in a sheet and in a beam, respectively. All instantaneous pictures of the system are produced with the Visual Molecular Dynamics (VMD) program [11]

In the present paper expressions from the reactive empirical form of potential, which takes into account the bond order (REBO) [17], are used for functions $V_R(r_{ij})$ and $V_A(r_{ij})$. They give improved values for elastic properties of diamond and graphite and more realistically simulate the short-range repulsions in comparison with an old version of the potential [17, 19]. For simplicity the term of the bond order \bar{B}_{ij} is chosen from the first version of the Brenner potential with parameters for the potential II in [16]. In the present work all splines were calculated with the code from TREMOLO [18], and forces were determined by the algorithm based on the linked cell list [14, 15, 18]. TREMOLO is the program tool with an open source code implemented in C++ in the Bohn University for simulation by the MD method.

Atoms in a beam do not interact with each other. Interaction of the beam particles with the sheet atoms are described by the Lennard-Jones potential:

$$u_{LJ} = \begin{cases} 4\varepsilon \left[\left(\frac{\sigma}{r_{ij}} \right)^{12} - \left(\frac{\sigma}{r_{ij}} \right)^6 \right], & r_{ij} \leq r_c, \\ 0, & r_{ij} > r_c \end{cases} \quad (2)$$

where $\sigma = 0,167$ nm; $\varepsilon = 0,5$ meV; the cut-off radius is $r_c = 0,9018$ nm. The mass of carbon atoms equals $19,9441 \cdot 10^{-27}$ kg.

Classical equations of motion are integrated using the Verlet method [14, 15] with the time step 0,1 fsec. Most of computer experiments were carried out within the microcanonical statistical ensemble, i.e., the total system energy E_{tot} , the number of particles N , and the volume V were fixed. To study the influence of heat dissipation on system behavior the conditions approximate to the canonical ensemble were considered as well, by a heat abstraction with the Berendsen thermostat [12, 15] coupled with the layer atoms. For its realization the technique described in [15] was used, where the atom velocities every 10 steps were multiplied by the value

$$\beta_\gamma = \left(1 + \gamma \left[\frac{T^D}{T(t)} - 1 \right] \right)^{1/2}, \quad (3)$$

where $T(t)$ and T^D are the current and the necessary temperatures, respectively; $\gamma \in [0;1]$ is the friction coefficient defining the coupling force between the thermostat and the system. The closer γ to 1, the stronger heat abstraction from the system. In the present paper we used $\gamma = 0,4$ corresponding to the rather strong coupling of the graphene atoms with the thermostat. Since the thermostat is connected with the sample only and the energy emission of beam atoms is not taken into account, strictly speaking the simulation conditions concerned are not the canonical ones in the presence of the thermostat. However, in the sequel we will use the expression ‘‘canonical ensemble’’ for brevity, keeping in mind the true simulation conditions.

The process of irradiation was proceeding as follows. During the first 1000 time steps (or 0,1 picoseconds) the system was equilibrated at the temperature 298 K, and in this case the vertical distance between the lower layer in a beam and a graphene sheet was 1,9895 nm, 1,9374 nm, and 1,9026 nm for $a = 0,3165$ nm, 0,2374 nm and 0,1582 nm, respectively. Then the impulse p , which is determined by the kinetic energy E :

$$p = \sqrt{2mE} \quad (4)$$

(m is the mass of carbon atom), was imparted to the beam particles along the negative z direction. Particles started moving toward the sample with the constant speed. We investigated the following values of the kinetic energy of atoms in a beam: 50, 100, 250, 500, and 1000 meV for conditions of the microcanonical ensemble, and 500 and 1000 meV in the presence of the thermostat for all values of the beam density. For the maximal value of kinetic energy (1000 meV) the particle velocity was about 4000 m/sec that allowed to use classical mechanics without relativistic corrections. The total simulation duration varied from 1 picosecond to 3,2 picoseconds depending on the energy of irradiating carbon atoms.

In numerical simulations we measured the system potential energy, the mechanical stresses arising in a graphene sheet, its deformation along the z -axis, and the atom coordinates were saved every 50 time steps that allowed to visualize the system behavior with the VMD program [11]. System potential energy E_{pot} was taken equal to the sum of potential energies of each particle, which contain both the binding energy of carbon atoms in graphene and their interaction energy with the beam particles.

Mechanical stresses in the carbon layer were calculated with the following expression for the stress tensor [18]:

$$\sigma^{\alpha\beta} = \frac{1}{V} \sum_{i=1}^N \left(m_i u_i^\alpha u_i^\beta + 0,5 \sum_{j=1, j \neq i}^N F_{ij}^\alpha r_{ij}^\beta \right), \quad (5)$$

where α and β denote direction in the Cartesian coordinate system (x , y , or z); u_i^k is the velocity of the i -th atom along the k -th direction; V is the volume of a graphene sheet (this is the product of the sample area by the length of atomic bonding in graphene, which is equal to 0,142 nm); m_i is the mass of carbon atom; N is the number of carbon atoms; F_{ij}^α and r_{ij}^β are the components of the force and the radius-vector between the i -th and the j -th atoms, respectively. In the present paper we calculated only the component σ^{zz} of the stress tensor along the direction of a beam motion, i.e., $\alpha, \beta = z$.

Straining of the sample is non-uniform during the interaction with the beam, and the spatial distribution of deformation over the sheet should be determined in order to characterize changes its shape. But for simplicity we measure the change of the carbon layer size along the z -axis only, and for its quantitative characteristic the maximal distance between carbon atoms along this direction is calculated. We consider only the absolute value of this quantity, and henceforth we will term it the deformation for brevity and denote as Δz .

3. RESULTS AND DISCUSSION

3.1 Microcanonical ensemble

In Fig. 2 we represent the time dependences of the stresses in a sheet and its deformation for the constant N , V , and E_{tot} and $a = 0,3165$ nm.

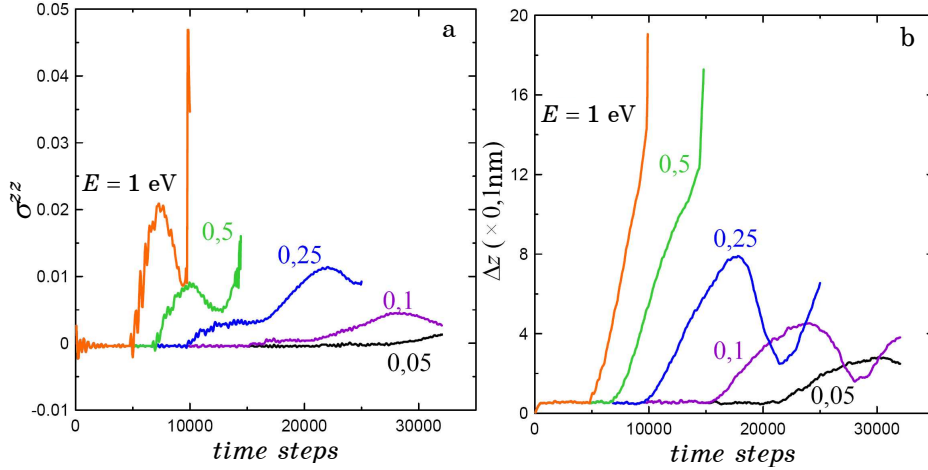


Fig. 2 – Time dependences of the stresses (a) and the deformation (b) of a graphene sheet for $a = 0,3165$ nm

Dependences obtained can be divided into two groups: in the first one the sample is not destroyed (beam energy is less than 0,5 eV), for the second group the energy of irradiating particles is enough for bond breaking in a sheet and, correspondingly, for its destruction. Let us consider in details the cases $E = 0,1$ and 0,5 eV as two possible scenarios of the system behavior.

At $E = 0,1$ eV particles reach the sample approximately after 15000 time steps that is manifested in the increase of the deformation (which is the absolute value of the maximal distance between atoms in a sheet along the z -axis) and stress (see point A in Fig. 3, 4). The largest “strain” of a graphene layer occurs at point B , and in this case a sheet starts moving as a whole in a downward direction, since it is not fixed in a space and the sheet bending changes the direction (atoms in a center start moving in an upward direction), that is exhibited in further decrease of deformation to point C . Non-linear relation between σ^{zz} and Δz can be explained by the following: the value of total stresses is determined not so much by the atom deviation along the vertical axis as by a number of atoms, which are reached by the excitation of beam particles. The stress maximum at point C corresponds to the moment when the majority of atoms have “sensed” the beam action.

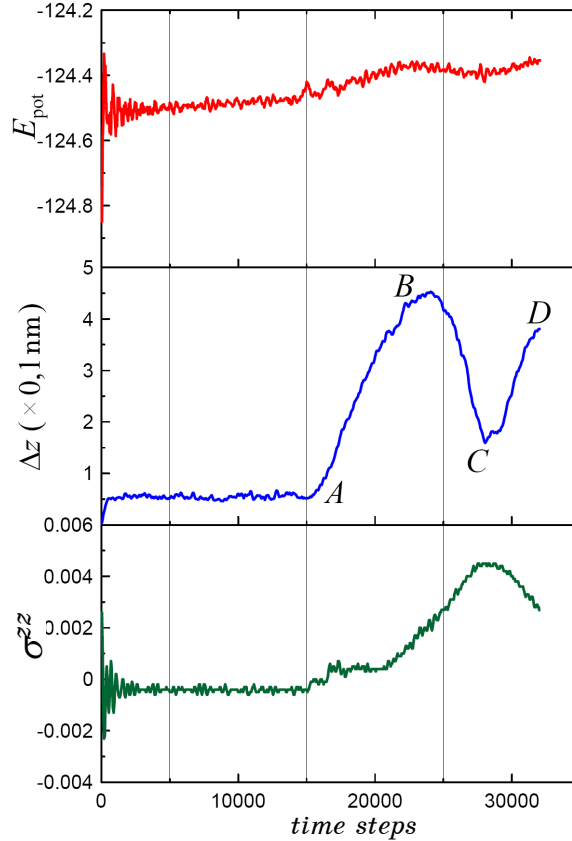


Fig. 3 – Time dependences of the system potential energy (per one atom), deformation and stresses for $E = 0,1$ eV and $a = 0,3165$ nm

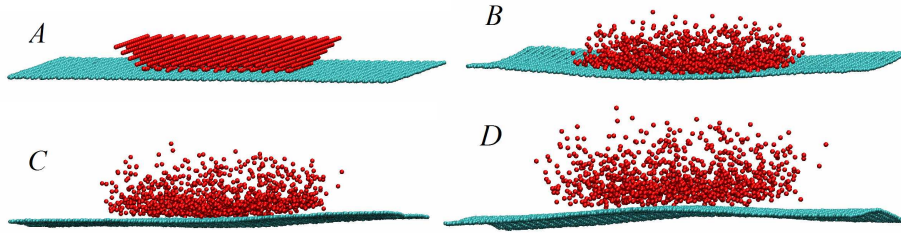


Fig. 4 – Instantaneous pictures of the system corresponding to the marked in Fig. 3 points

It is seen from Fig. 3, 4 that the particle energy $E = 0,1$ eV is not enough for bond breaking in the sample, and elastic scattering of particles occurs. And all the atoms are reflected and none of them penetrates through a sheet.

For $E = 0,5$ eV particles collide with the sheet after 7000 steps (point A in Fig. 5, 6). It is seen, that the stresses rather quickly, in fact, linearly, increase with the deformation growth reaching the maximum at point B. The stress falling in the section BC is explained by the stress redistribution all over a sheet. Note, that in contrast to the previous case the steady deformation increase is observed here, that points at the sample depression by a beam in one direction (downward). After reaching the stress minimum at point C the sheet starts moving as a whole in a downward direction, and stresses grow achieving the value, which is enough for bond breaking. The sample destruction occurs, which is exhibited in the jumps of stresses and in the sharp increase of Δz and E_{pot} as well. The difference from the previous case is evident, where the absence of sufficient changes in the potential energy was observed (see Fig. 3), and the particle penetration through the sheet before its destruction also takes place, as seen from Fig. 6.

Diagrams for other values of the potential energy of a beam (represented in Fig. 2) can be explained in the same way.

Note, that unambiguous comparison of results obtained both in the present work and in [9, 10] is impossible. This is connected with the following: in [9, 10] the chemical reactions and absorption of hydrogen isotopes by the sample are possible due to using the Brenner potential for irradiating particles. This occurs in the particle energy range 0,5-15 eV [9]. For energies more than 15 eV particles penetrate through a graphene sheet not being absorbed and not destroying the sample [9]. Lower energies of irradiating particles enough for graphene destruction obtained within this work, can be explained by the expression from the first version of the Brenner potential for the term of the bond order \bar{B}_{ij} in (1) that could lead to the weaker covalent bonds in a sample.

Time dependences of the stresses σ^{zz} and the deformation Δz for $a = 0,2374$ nm have the same behavior, and, therefore, the same explanation as for $a = 0,3165$ nm (Fig. 7). We only note that the large beam density promotes the greater maximal tension of a sheet, that is seen from the figures for deformation.

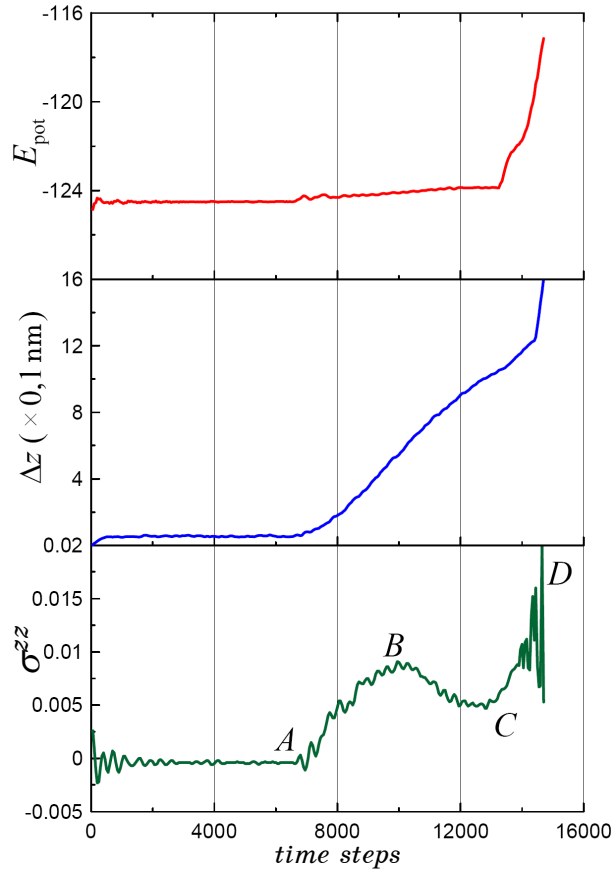


Fig. 5 – Time dependences of the system potential energy (per one atom), deformation and stresses for $E = 0,5 \text{ eV}$ and $a = 0,3165 \text{ nm}$

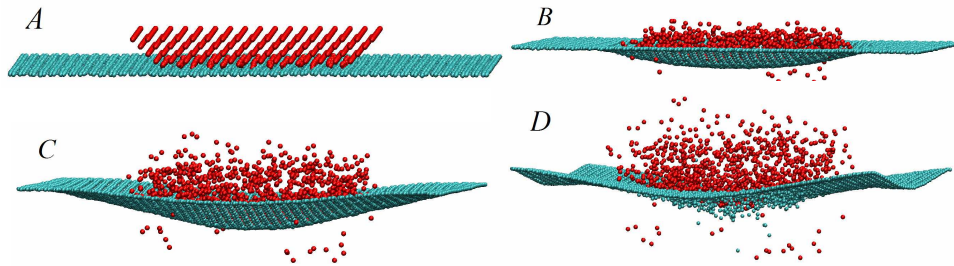


Fig. 6 – Instantaneous pictures of the system corresponding to the marked in Fig. 5 points

Atomic configurations of the system for $a = 0,2374 \text{ nm}$ and $E = 0,5 \text{ eV}$ in different time moments are given in Fig. 8. It is seen, that the particle penetration through the sample before its destruction takes place, as in the previous case. We also have to note, that the large beam density leads to more intensive destruction, that is exhibited in pronounced jumps of stresses on the corresponding dependence (Fig. 7a) as well.

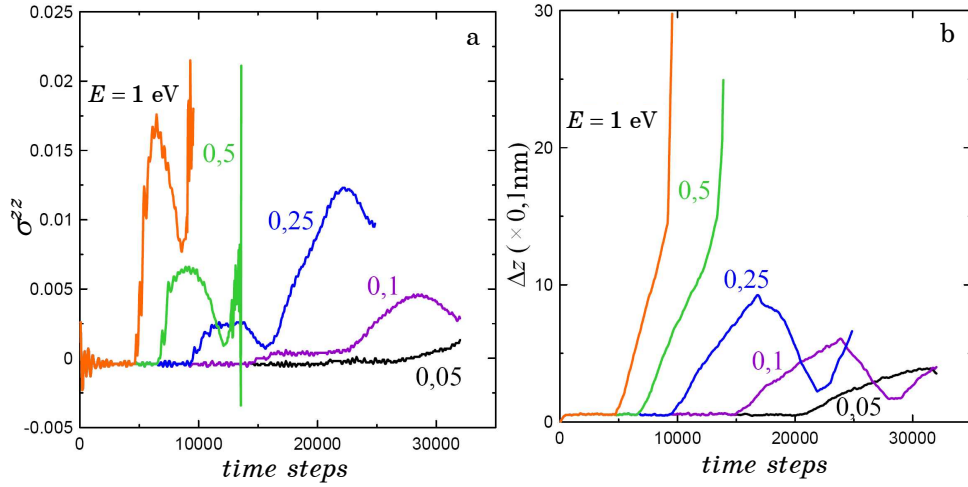


Fig. 7 – Time dependences of the stresses (a) and the deformation (b) of a graphene sheet for $a = 0,2374 \text{ nm}$ in conditions of the microcanonical ensemble

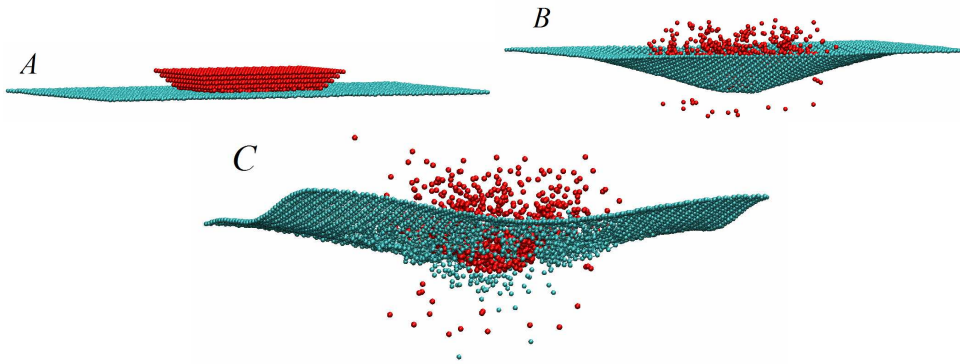


Fig. 8 – Instantaneous pictures of the system for $E = 0,5 \text{ eV}$ and $a = 0,2374 \text{ nm}$: A – 6750, B – 12250, C – 14450 time steps

Time dependences of the stresses σ^{zz} and the deformation Δz for $a = 0,1582 \text{ nm}$ (Fig. 9) are the same as for two previous cases. The greater jumps of stresses are observed, which indicate more intensive destruction that can be seen in Fig. 10 as well.

3.2 Canonical ensemble

Up to now we have considered conditions of the microcanonical statistical ensemble, i.e., the total system energy E_{tot} , the volume V , and the number of particles N were fixed. But practically the system is always open and there is a heat abstraction from it. In our case cooling is intensified by the small sample thickness [20]. To take into account the mentioned factors we have carried out some computer experiments, in which the sheet cooling was provided by the Berendsen thermostat [15].

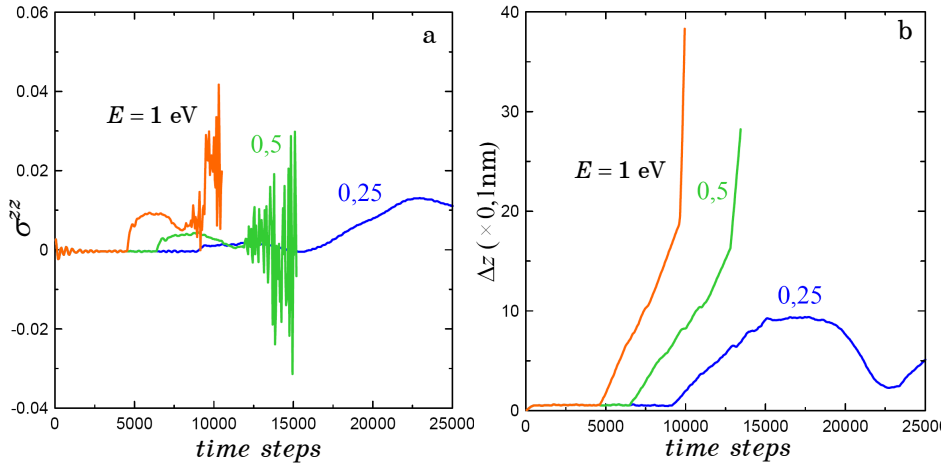


Fig. 9 – Time dependences of the stresses (a) and the deformation (b) of a graphene sheet for $a = 0,1582$ nm

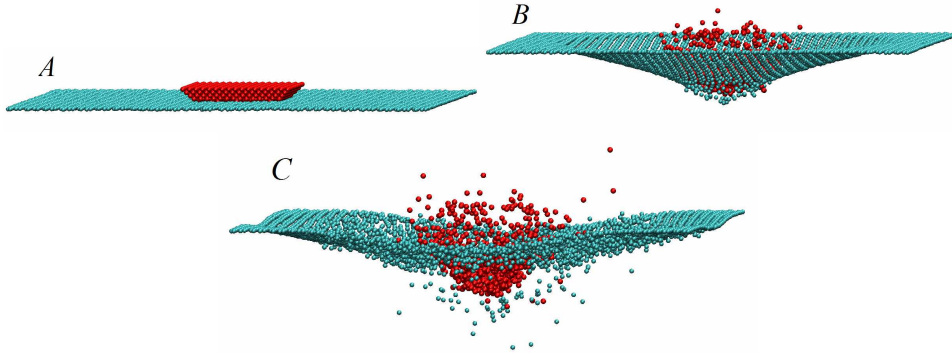


Fig. 10 – Instantaneous pictures of the system for $E = 0,5$ eV and $a = 0,1582$ nm: A – 6750, B – 12250, C – 14450 time steps

Time dependences of the stresses σ^{zz} and the deformation Δz at $E = 0,5$ eV (for $E = 1$ eV we have obtained the same results, which are not shown here) represented in Fig.11 have the qualitatively similar behavior for all three values of the particle density in a beam.

Presence of the thermostat leads to the situation that now for energy, at which the sample destruction occurred in conditions of microcanonical ensemble, the particle elastic scattering takes place that can be also seen from Fig. 12, where the instantaneous pictures of the system for $a = 0,3165$ nm are represented. The absence of sample destruction is confirmed by the curve shape, which has two maximums for the stresses, and one maximum for the deformation, that is similar to the case of small particle energies considered in the previous subsection. Therefore the explanation of system behavior is also the same as considered in 3.1.

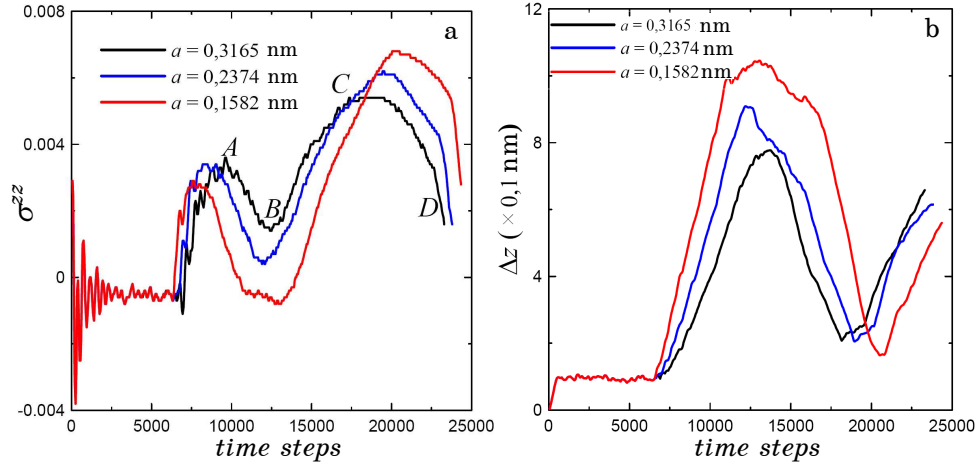


Fig. 11 – Time dependences of the stresses (a) and the deformation (b) of a graphene sheet at $E = 0,5$ eV for different beam densities in conditions of the microcanonical ensemble

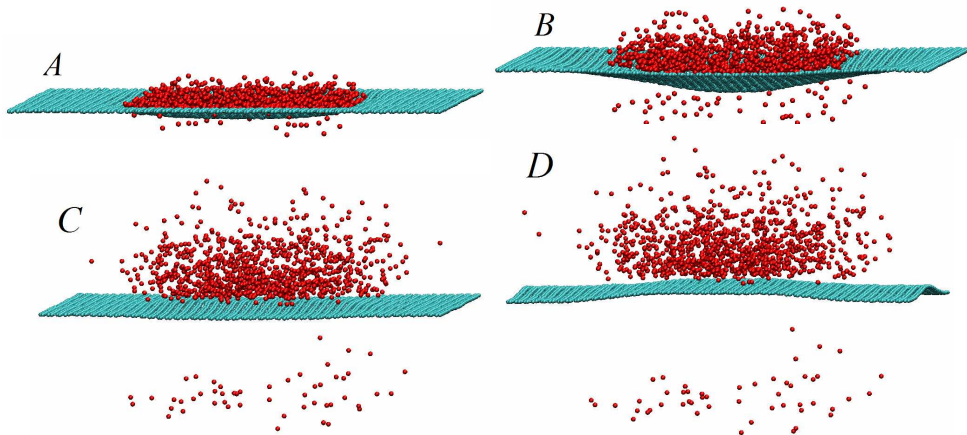


Fig. 12 – Instantaneous pictures of the system corresponding to the marked in Fig. 11a points

Let us briefly analyze the system behavior for different particle densities in a beam. Increase of the particle density (or decrease of a) leads to the narrowing of the first stress maximum, decrease of its height, and deepening of the next minimum. For lesser a the higher second stress maximum is observed that indicates the stress increase with the growth of the particle density. In this case the larger “punching” of a sample takes place that is exhibited in increase of the maximal deformation with the a decrease (see Fig. 11b).

Thus, the connection of a graphene sheet with the thermostat promotes the sample ability to endure higher beam energies not being failed. In other words, heat abstraction shifts the energy value, at which the sample destruction occurs, toward the higher values.

4. CONCLUSIONS

Classical MD simulations of the bombardment of a graphene sheet by a beam of carbon atoms are carried out. The main results are the following:

- in conditions of the microcanonical ensemble there is a value of particle energy (it is approximately equal to 0,5 eV), which overriding leads to the sample destruction, that is exhibited in jumps of stresses and in abrupt increase of the deformation and the system potential energy. More intensive destruction is observed for lesser a ;
- time dependences of the stresses and the deformation in NVE conditions at low energies have qualitatively equal behavior for all beam densities. Quantitatively larger densities condition the larger sample deformation;
- heat abstraction from the system induces the shift of the beam energy (at which the sample destruction occurs) toward the higher values;
- beam density in the presence of the thermostat does not qualitatively influence on the shape of time dependences of the stresses and the deformation. Increase of the beam density causes the growth of the maximal stress value in a sheet. In this case the larger “punching” of the sample takes place that is exhibited in increase of the maximal deformation.

We acknowledge the Fundamental Researches State Fund of Ukraine and the Russian Foundation for Basic Research (Grant No. F28/443-2009) for support.

REFERENCES

1. K.S. Novoselov, A.K. Geim, S.V. Morozov, D. Jiang, Y. Zhang, S.V. Dubonos, I.V. Grigorieva, A.A. Firsov, *Science* **306**, 666 (2004).
2. K.S. Novoselov, A.K. Geim, S.V. Morozov, D. Jiang, M.I. Katsnelson, I.V. Grigorieva, S.V. Dubonos, A.A. Firsov, *Nature* **438**, 197 (2005).
3. Y. Zhang, J.W. Tan, H.L. Stormer, P. Kim, *Nature* **438**, 201 (2005).
4. A.H. Castro Neto, F. Guinea, N.M.R. Peres, K.S. Novoselov, A.K. Geim, *Rev. Mod. Phys.* **81**, 109 (2009).
5. K.S. Novoselov, D. Jiang, F. Schedin, T.J. Booth, V.V. Khotkevich, S.V. Morozov, A.K. Geim, *P. Natl Acad. Sci. USA* **102**, 10451 (2005).
6. A.K. Geim, K.S. Novoselov, *Nat. Mater.* **6**, 183 (2007).
7. J.C. Meyer, A.K. Geim, M.I. Katsnelson, K.S. Novoselov, T.J. Booth, S. Roth, *Nature* **447**, 60 (2007).
8. M.H. Gass, U. Bangert, A.L. Bleloch, P. Wang, R.R. Nair, A.K. Geim, *Nat. Nanotechnol.* **3**, 676 (2008).
9. H. Nakamura, A. Takayama, A. Ito, *Contrib. Plasm. Phys.* **48**, 265 (2008).
10. A. Ito, H. Nakamura, *Thin Solid Films* **516** No19, 6553 (2008).
11. W. Humphrey, A. Dalke, K. Schulten, *J. Mol. Graphics* **14** No1, 33 (1996).
12. S.J. Heo, S.B. Sinnott, D.W. Brenner, J.A. Harrison, *Nanotribology and nanomechanics*, 623 (Berlin: Springer: 2005).
13. M.P. Allen, D.J. Tildesley, *Computer Simulation of Liquids* (Oxford: Clarendon Press: 1995).
14. D.C. Rapaport, *The art of molecular dynamics simulation, 2nd ed.* (Cambridge: Cambridge University Press: 2004).
15. M. Griebel, S. Knapek, G. Zumbusch, *Numerical simulation in molecular dynamics* (Berlin, Heidelberg: Springer: 2007).
16. D.W. Brenner, *Phys. Rev. B* **42** No15, 9458 (1990).

17. D.W. Brenner, O.A. Shenderova, J.A. Harrison, S.J. Stuart, B. Ni, S.B. Sinnott, *J. Phys.-Condens. Mat.* **14**, 783 (2002).
18. A. Caglar, M. Griebel, *Molecular dynamics on parallel computers*, 1 (Julich: World Scientific: 1999).
19. J.A. Harrison, D.W. Brenner, C.T. White, R.J. Colton, *Thin Solid Films* **206**, 213 (1991).
20. R.P. Feynman, *Eng. Sci.* **23**, 22 (1960) (see <http://www.zyvex.com/nanotech/feynman.html>).